Topological Waves in Fluids with Odd Viscosity

Anton Souslov,[1,2,*] Kinjal Dasbiswas,[1,3] Michel Fruchart,[1]
Suriyanarayanan Vaikuntanathan,[1,4] and Vincenzo Vitelli[1,5,†]

[1]*The James Franck Institute, The University of Chicago, Chicago, Illinois 60637, USA*
[2]*Department of Physics, University of Bath, Bath BA2 7AY, United Kingdom*
[3]*Department of Physics, University of California, Merced, Merced, California 95343, USA*
[4]*Department of Chemistry, The University of Chicago, Chicago, Illinois 60637, USA*
[5]*Department of Physics, The University of Chicago, Chicago, Illinois 60637, USA*

Fluids in which both time reversal and parity are broken can display a dissipationless viscosity that is odd under each of these symmetries. Here, we show how this odd viscosity has a dramatic effect on topological sound waves in fluids, including the number and spatial profile of topological edge modes. Odd viscosity provides a short-distance cutoff that allows us to define a bulk topological invariant on a compact momentum space. As the sign of odd viscosity changes, a topological phase transition occurs without closing the bulk gap. Instead, at the transition point, the topological invariant becomes ill defined because momentum space cannot be compactified. This mechanism is unique to continuum models and can describe fluids ranging from electronic to chiral active systems.

In ordinary fluids, acoustic waves with sufficiently large wavelength have arbitrarily low frequency due to Galilean invariance [1]. When either a global rotation or an external magnetic field is present, Galilean invariance is explicitly broken by either Coriolis or Lorentz forces within the fluid, respectively. Hence, the spectrum of acoustic waves becomes gapped in the bulk. Yet, a peculiar phenomenon can occur at edges or interfaces: chiral edge modes propagate robustly irrespective of interface geometry. This phenomenon analogous to edge states in the quantum Hall effect [2–4] was unveiled in the context of equatorial waves [5] and explored in out-of-equilibrium and active fluids [6,7]. Similar phenomena occur in lattices of circulators [8,9], polar active fluids under confinement [10], and coupled mechanical oscillators [11–13], including gyroscopes [14,15] and oscillators subject to Coriolis forces [16,17].

In addition to Coriolis or Lorentz body forces, fluids in which time reversal and parity are broken generically exhibit a dissipationless viscosity that is odd under each of these symmetries [18,19]. The viscosity tensor η_{ijkl} relates the strain rate $v_{kl} \equiv \partial_k v_l$ to the viscous part of the stress tensor $\sigma_{ij} = \eta_{ijkl} v_{kl}$. Odd viscosity refers to the antisymmetric part of the viscosity tensor $\eta^o_{ijkl} = -\eta^o_{klij}$ [18,19]. In an isotropic two-dimensional fluid, odd viscosity is specified by a single pseudoscalar η^o; see Supplemental Material (SM) for details [19,20]. Odd viscosity changes sign under either time reversal or parity, and hence must vanish when at least one of these symmetries is present. Conversely, odd viscosity is generically nonvanishing as soon as both time reversal and parity

are broken [21–23]. For instance, microscopic Coriolis or Lorentz forces are sufficient to induce a nonzero odd viscosity [24,25], in addition to the corresponding body forces. Odd viscosity has been studied theoretically in various systems (see SM for a partial review [20]) including polyatomic gases [26], magnetized plasmas [25,27], fluids of vortices [28–31], chiral active fluids [32], quantum Hall states, and chiral superfluids or superconductors [33–43]. Its presence has been experimentally reported in polyatomic gases [44–46] (where both positive and negative odd viscosities were observed under the same magnetic field, for different molecules), electron fluids subject to a magnetic field [47], and spinning colloids [48].

Here, we show that the presence of odd viscosity fundamentally affects the topological properties of linear waves in the fluid. In particular, the net number of chiral edge states depends on the signs of both odd viscosity and the external magnetic field (or rotation) on each side of an interface. We define a bulk topological invariant that accounts for this striking behavior. In a fluid, momentum space is not compact (linear momentum can be arbitrarily large). Hence, the definition of bulk topological invariants requires a constraint at short wavelengths [49–51]. We show that a nonvanishing odd viscosity provides such a short-distance cutoff, associated with microscopic angular momenta (see Fig. 1). Upon changing the sign of odd viscosity, a topological phase transition occurs without gap closing because at the transition, the small-wavelength constraint changes, so the topological invariant becomes ill defined. When odd viscosity goes to 0, half of the edge states are no longer hydrodynamic because their
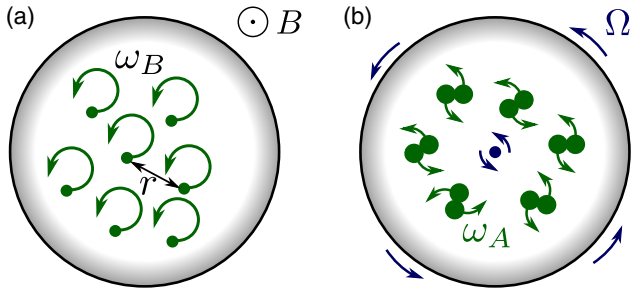
FIG. 1. Physical realizations of the minimal model for topological fluids with odd viscosity. (a) Two-dimensional plasma under magnetic field B, with cyclotron frequency $\omega_B = qB/M$. (b) Chiral active fluid with intrinsic rotation angular frequency ω_A, subject to a global rotation with angular frequency $\omega_B = -2\Omega$.

penetration depths vanish while the other half retain a finite penetration depth set by the gap size.

Model.—Consider the odd Navier-Stokes equations describing a compressible time-reversal and parity violating fluid,

$$\partial_t \rho(\mathbf{r}, t) = -\rho_0 \nabla \cdot \mathbf{v}(\mathbf{r}, t) \qquad (1)$$

$$\partial_t \mathbf{v} = -c^2 \nabla \rho / \rho_0 + \omega_B \mathbf{v}^* + \nu^o \nabla^2 \mathbf{v}^*, \qquad (2)$$

where $\mathbf{r} \equiv (x, y)$ is the position, ρ is the fluid density whose average is ρ_0 [52], $\mathbf{v} \equiv (v_x, v_y)$ is the velocity, and $\mathbf{v}^* \equiv (v_y, -v_x)$ is the velocity rotated by 90°. The chiral body force $\omega_B \mathbf{v}^*$ can arise, e.g., from (i) Lorentz forces for which $\omega_B = qB/M$ where $B\hat{z}$ is the magnetic field, q is particle charge, and M is particle mass or (ii) Coriolis forces for which $\omega_B = -2\Omega$ where $\Omega\hat{z}$ is the rotation field. Besides the body force $\omega_B \mathbf{v}^*$, the Lorentz or Coriolis forces experienced by the fluid particles also give rise to an odd viscosity term $\nu^o \nabla^2 \mathbf{v}^*$; see SM [20] and Refs. [24,25] for kinetic theory derivations and the dependence of odd viscosity on fluid parameters, including temperature. Other microscopic mechanisms violating both time reversal and parity also contribute to the odd viscosity. This is for instance the case with active torques (see SM [20] and Ref. [32]).

Equations (1) and (2) are our starting point. Equivalent equations, but with zero odd viscosity and with ρ replaced by the height of a surface wave, are studied in the context of geophysics [53–58]. The topological properties of such waves were identified for fluids on a sphere [5]; see also Ref. [6]. In the next section, we show that a nonzero odd viscosity allows the topological characterization of density waves for fluids within a plane by acting as a short-distance cutoff; see also Ref. [59]. By contrast, an ordinary viscosity term $\nu \nabla^2 \mathbf{v}$ by itself does not lead to a regularization of the continuum theory; this term can be neglected in the limit $\nu^o / \nu \gg 1$ (see SM [20] for a discussion).

Bulk dispersion and topology.—In the fluid bulk, Eqs. (1) and (2) can be replaced by their momentum-space version $\partial_t [\rho, \mathbf{v}] = i \mathcal{L}(\mathbf{q}) [\rho, \mathbf{v}]$ where the operator $\mathcal{L}(\mathbf{q}) \equiv q_x \Lambda_x + q_y \Lambda_y + (\omega_B - \nu^o q^2) \Lambda_z$ is expressed in terms of the 3×3 matrices Λ_i ($i = x, y, z$; see SM for definitions [20]). Here, $\rho(\mathbf{q}, t), \mathbf{v}(\mathbf{q}, t)$ are the Fourier transforms of $\rho(\mathbf{r}, t), \mathbf{v}(\mathbf{r}, t)$, and the wave vector $\mathbf{q} \equiv (q_x, q_y)$ takes values in the entire plane. The dispersion relations $\omega_s(\mathbf{q})$ for the frequency of bulk modes are the eigenvalues of $\mathcal{L}(\mathbf{q})$ and consist of three branches. One branch has a flat dispersion $\omega_0(\mathbf{q}) = 0$ with an eigenmode combining vorticity and density (see SM [20]). The acoustic spectrum is described by the other two branches, with dispersion relations

$$\omega_\pm(\mathbf{q})/\omega_B = \pm\sqrt{(1 - m\bar{q}^2)^2 + \bar{q}^2}, \qquad (3)$$

where $\bar{q} = |\mathbf{q}| c / \omega_B$. The qualitative features of these dispersion relations near $\bar{q} = 0$ depend on the frequency ω_B and the dimensionless velocity ratio $m \equiv \omega_B \nu^o / c^2$, which is analogous to the square of a Mach number (see SM [20]). As ω_B (and not ν^o) controls the magnitude of the gap at $\bar{q} = 0$, odd viscosity alone cannot open a gap in the spectrum of acoustic waves. However, m plays an important role in the shape of the dispersion relation. For $m < 1/2$, the band structure looks similar to the case $m = 0$; see Figs. 2(a)–2(c). For $m > 1/2$, the band structure resembles a Mexican-hat potential. While the separation between the bands is unchanged at $\bar{q} = 0$, the gap is now located along a circle with radius $\bar{q} = \text{const} \neq 0$, and the gap size decreases scaling as $\omega_B m^{-1/2}$ at large m. In this regime, the group velocity $\partial \omega_+ / \partial q$ of sound waves in the fluid is negative for $0 < \bar{q} < \sqrt{(2m - 1)/(2m^2)}$, a feature shared with left-handed metamaterials, which have a negative index of refraction.

The analogy between acoustic waves on top of a constant background vorticity and the quantum-mechanical wave function of electrons in a constant magnetic field suggests that Eqs. (1) and (2) can lead to topological phenomena akin to the quantum Hall effect. The geometric phases in the wave propagation are captured by the Berry curvature $F_\pm(\mathbf{q}) = \nabla_\mathbf{q} \times [(u_\mathbf{q}^\pm)^\dagger \cdot \nabla_\mathbf{q} u_\mathbf{q}^\pm]$ of the eigenmodes $u_\mathbf{q}^\pm$ associated with the $\pm$ bands at $\mathbf{q}$ in Eq. (3), which reads

$$F_\pm(\bar{q}) = \mp \frac{1 + m\bar{q}^2}{[\bar{q}^2 + (1 - m\bar{q}^2)^2]^{3/2}}. \qquad (4)$$

In the usual case, the integral of Berry curvature over momentum space is equal to a topological invariant. However, standard topological materials have a lattice structure, for which the wave vector $\mathbf{q}$ lives in a compact Brillouin zone, equivalent to a torus. In contrast, fluid models such as the one described by Eqs. (1) and (2) do not include a short-distance cutoff, and the wave vector spans the entire two-dimensional (q_x, q_y) plane. As a consequence, the definition
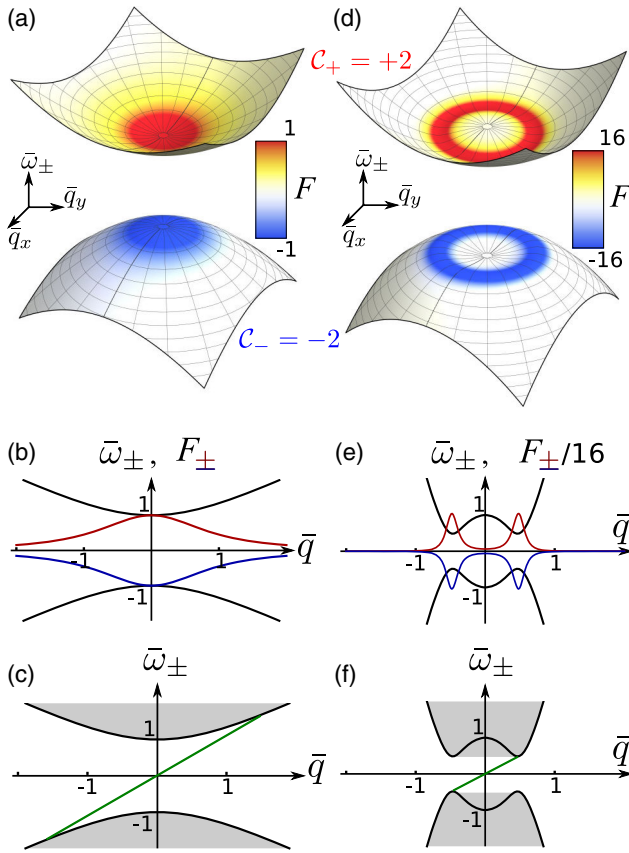
FIG. 2. Effect of large odd viscosity on the topological band structure. (a) Frequency $\bar{\omega}_\pm \equiv \omega_\pm(\mathbf{q})/\omega_B$ and Berry curvature $F_\pm$ for $m = 0.1$. (c) Schematic representation of band structure for a system with edge. Gray regions of bulk states are connected by lines of edge states. [(d)–(f)] Same as (a)–(c), but for $m = 4$.

of topological invariants for fluid models requires the introduction of a constraint at small length scales [49–51,61–67], resulting in a nonzero m in Eq. (4). Formally, this addition can be seen as an ultraviolet regularization of the continuum model. Here, a mesoscopic length scale naturally arises from odd viscosity whose presence leads to a well-defined limit for $\mathcal{L}(\mathbf{q})$ as $|\mathbf{q}| \to \infty$, independent of the direction of $\mathbf{q}$. As a result, integer-valued topological invariants can be associated to each band of the wave spectrum as the first Chern numbers of a modified version of the operator $\mathcal{L}$ defined over the compactified momentum space, i.e., a sphere (see SM [20] and Refs. [49–51,61–67] in which a different short-distance cutoff is considered in other physical contexts).

When both ω_B and ν^o are nonzero (and only in this case), the first Chern number $\mathcal{C}_-$ of the band with dispersion ω_- is given by

$$\mathcal{C}_- = \text{sign}(\nu^o) + \text{sign}(\omega_B), \qquad (5)$$

whereas the other acoustic band has the opposite first Chern number $\mathcal{C}_+ = -\mathcal{C}_-$, and the flat band $\omega = 0$ has a

vanishing first Chern number. When odd viscosity vanishes, $\mathcal{L}(\mathbf{q})$ does not have a unique limit as $|\mathbf{q}| \to \infty$. Hence, the compactification is no longer possible, and the Chern numbers become ill defined. Remarkably, this results in a topological phase transition without gap closing [50,62,63]. This phase transition is due to an ultraviolet divergence of the hydrodynamic field theory. In other words, the hydrodynamic description of the system breaks down as the small length scales associated with odd viscosity vanish.

The distribution of Berry curvature is also qualitatively modified by odd viscosity (see Fig. 2). When $0 < m < 3/8$, the Berry curvature concentrates at $\bar{q} = 0$. At higher values $m > 3/8$, the Berry curvature concentrates on a ring with finite radius, scaling as $\bar{q} \sim m^{-1/2}$ for large m. For negative m, a peak at $\bar{q} = 0$ coexists with an extremum along a ring, with opposite contribution.

Bulk-boundary correspondence.—Topological invariants characterize infinite systems without boundaries, but their values are usually related to observable phenomena at interfaces. According to bulk-boundary correspondence, the net number of chiral edge states (with frequencies in the bulk band gap) expected at an interface between two systems L and R with invariants $\mathcal{C}_-^{L/R}$, respectively, is $N = \mathcal{C}_-^L - \mathcal{C}_-^R$. Note that the general validity of bulk-boundary correspondence has not been established in continuum fluid models. We assume that the case of a container wall can be considered by setting $\mathcal{C}_-^R = 0$ for the region where waves cannot propagate [4,68]. Provided that both ω_B and ν^o are nonzero, Eq. (5) applied to the region where waves propagate implies that a chiral fluid has a total of two protected edge modes traveling in the same direction at an edge if $\omega_B \nu^o > 0$ (corresponding to $|\mathcal{C}_-^L| = 2$), or a net total of zero chiral edge modes if $\omega_B \nu^o < 0$ (corresponding to $\mathcal{C}_-^L = 0$). Notably, a topological phase transition occurs between these two regimes without closing the bulk band gap. Here, the second case corresponds to two counterpropagating edge states that are not topologically protected (see SM [20] and the supplementary movie). We demonstrate these phenomena within finite-element simulations of Eqs. (1) and (2) in a modified disk geometry using COMSOL MULTIPHYSICS (see Fig. 3, SM [20], and the supplementary movies). The density wave at the edge is excited at a frequency in the gap (cf., Fig. 2). For a range of model parameters with $\omega_B \nu^o > 0$, the edge waves propagate unidirectionally around the edge of the disk and do not scatter off sharp corners and prominent defects. Similarly, an interface between fluids with opposite ω_B with $\omega_B \nu^o > 0$ on both sides should exhibit four copropagating edge states. This is in sharp contrast to the case of strictly vanishing odd viscosity [5–7], where only two edge modes are present at an interface.

Although the existence of chiral edge states relies only on the nonzero topological invariant associated with the bulk bands, their penetration depth is determined by the
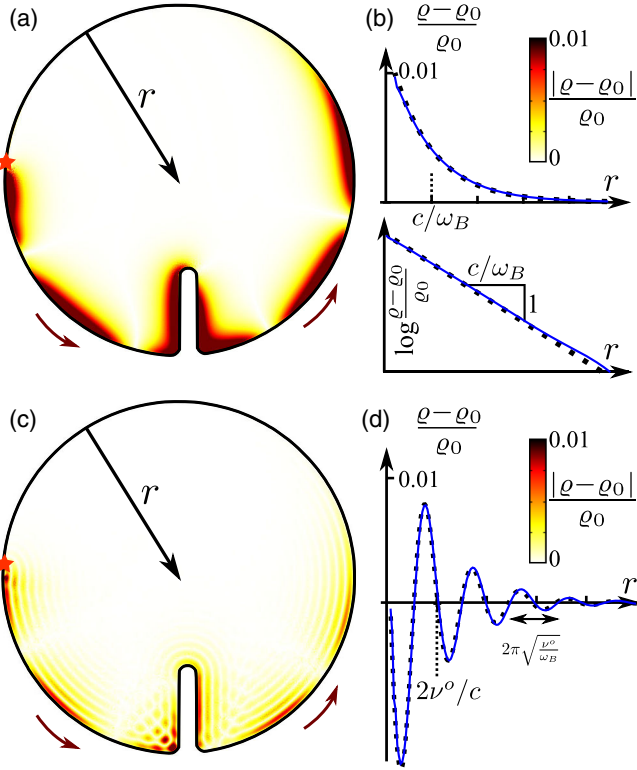
FIG. 3. Simulations showing topological edge states. (See the supplementary movie.) (a) Edge state with $m = 0.0625$. Color shows density deviations, $|\rho - \rho_0|/\rho_0$. The edge state is excited using small-frequency source (star, left). [(b), top] Radial profile of the chiral edge state in (a) comparing simulations and analytics. [(b), bottom] Same plot on log-linear scale. (c) Snapshot as in (a), but with $m = 9.0$. (d) Radial profile from (c) exhibits oscillations.

various parameters in Eqs. (1) and (2). The penetration depth depends on the separation between the two topological bands, which can scale with odd viscosity. To estimate this penetration depth κ^{-1}, we consider a simplified geometry with a straight fluid interface perpendicular to the y axis with a fluid described by Eqs. (1) and (2) filling the region $y < 0$, whereas the region $y > 0$ is empty. Along this edge, solutions for density waves in the fluid have the form $e^{i(\omega t - \mathbf{q} \cdot \mathbf{r}) + \kappa y}$ (for $y < 0$), which decays to 0 as $y \to -\infty$ for real ω, q_x, q_y and positive κ. We assume that the dispersion of the edge states goes through the point $\omega(q_x = 0) = 0$ (see SM for the general case [20]). From Eq. (3) where $\bar{\kappa} \equiv \kappa c/\omega_B$, we find

$$[[1 - m(\bar{q}_y + i\bar{\kappa})^2]^2 + (\bar{q}_y + i\bar{\kappa})^2]^{1/2} = 0. \quad (6)$$

For small odd viscosity with $0 < m < 1/4$, we find solutions with $\bar{q}_y = 0$ and $\kappa_\pm = (c \pm \sqrt{c^2 - 4\nu^o \omega_B})/2\nu^o$. This solution includes the case $\kappa_- \to \omega_B/c$ in the limit $\nu^o \to 0$ [5]. In this limit, $\kappa_+ \sim c/\nu^o \to \infty$, which implies this mode has vanishing penetration depth and therefore is no

longer hydrodynamic. By contrast, no solution satisfying $q_y = 0$ exists at large odd viscosity when $m > 1/4$. Instead, the edge wave has a profile whose amplitude both decays and oscillates away from the edge. When $m \gg 1$ this solution has the form $q_y = \pm\sqrt{\omega_B/\nu^o}$ and $\kappa = c/(2|\nu^o|) \sim m^{-1}\omega_B/c \ll \omega_B/c$. In Fig. 3, we compare these results with numerical simulations in which no-tangential-stress, no-penetration boundary conditions have been chosen (see SM [20] for details, where we also observe that no-slip boundary conditions do not lead to qualitative changes). We find good agreement between our theoretical predictions and numerical simulations for both the penetration depth [for ν^o both small, Fig. 3(b), and large, Fig. 3(d)] and the oscillation wavelength [for large ν^o, Fig. 3(d)].

Discussion.—When can odd viscosity be neglected? Comparing the magnitudes of terms on the right-hand side of Eq. (2), we find two length scales $\ell_1 \equiv \nu^o/c$ and $\ell_2 \equiv \sqrt{\nu^o/\omega_B}$ from the ratio of the compressibility and Lorentz or Coriolis terms to odd viscosity (see SM [20]). At scales significantly larger than $\ell_{1,2}$, odd viscosity is a small effect. When $\nu^o \to 0$, $\ell_{1,2}$ both vanish and the effects of odd viscosity are no longer captured by the hydrodynamic description. In this case, the lack of a cutoff at short wavelength in the band structure allows for a topological phase transition without a corresponding closing of the band gap. In a topological system with boundaries, the penetration depth of one of the edge states scales as ℓ_1 in the limit $\nu^o \to 0$, whereas the penetration depth of the other edge state converges to a finite value. In this limit, the effects of odd viscosity are confined in a boundary layer with small thickness of order ℓ_1, in which the hydrodynamic description does not apply. In particular, we find that in the limit of vanishing odd viscosity, a single edge state with finite penetration depth remains, with a chirality controlled by the sign of ω_B. The other edge state with vanishingly small penetration depth is either copropagating or counterpropagating, depending on the relative sign of ω_B and ν^o, but likely becomes unobservable in the limit of zero odd viscosity, in agreement with the results of Refs. [5–7].

When the length scales associated with odd viscosity are sufficiently large, both edge states should be observable, and different signs of odd viscosity relative to ω_B lead to physically distinct situations. Positive and negative $\omega_B \nu^o$ are possible even when the body force and odd viscosity both arise from the same origin. For instance, polyatomic gases under magnetic field can have an odd viscosity of either sign in the same magnetic field, depending on the constituent molecules [44–46]. Besides, active systems may allow one to control both quantities independently due to an additional internal source of time reversal and parity violation. For example, chiral active fluids consist of microscopic components of size a subject to internal torques and dissipation [69–91], resulting in a steady-state rotation of each microscopic component with frequency ω_A

and an odd viscosity $\nu^{o} \propto \omega_{A} a^{2}$ [32], where ω_{A} and ω_{B} can have opposite signs.

Note added in the proof.—Recently, we learned about Ref. [92], which examines topological bulk-boundary correspondence for electromagnetic waves in the continuum.

[*]a.souslov@bath.ac.uk
[†]vitelli@uchicago.edu
[1] The equations of motion of the fluid are invariant under the Galilean transformations $\mathbf{v}(x, t) \rightarrow \mathbf{v}(x, t) + \mathbf{v}_{0}$, where $\mathbf{v}(x, t)$ is the velocity field of the fluid particles and $\mathbf{v}_{0}$ an arbitrary uniform velocity field corresponding to an inertial frame. Hence, density waves with arbitrarily large wavelength (approaching a uniform flow) have vanishingly small frequency.
[2] K. v. Klitzing, G. Dorda, and M. Pepper, Phys. Rev. Lett. **45**, 494 (1980).
[3] D. J. Thouless, M. Kohmoto, M. P. Nightingale, and M. den Nijs, Phys. Rev. Lett. **49**, 405 (1982).
[4] M. Z. Hasan and C. L. Kane, Rev. Mod. Phys. **82**, 3045 (2010).
[5] P. Delplace, J. B. Marston, and A. Venaille, Science **358**, 1075 (2017).
[6] S. Shankar, M. J. Bowick, and M. C. Marchetti, Phys. Rev. X **7**, 031039 (2017).
[7] K. Dasbiswas, K. K. Mandadapu, and S. Vaikuntanathan, Proc. Natl. Acad. Sci. U.S.A. **115**, E9031 (2018).
[8] R. Fleury, D. L. Sounas, C. F. Sieck, M. R. Haberman, and A. Alù, Science **343**, 516 (2014).
[9] A. B. Khanikaev, R. Fleury, S. H. Mousavi, and A. Alù, Nat. Commun. **6**, 8260 (2015).
[10] A. Souslov, B. C. van Zuiden, D. Bartolo, and V. Vitelli, Nat. Phys. **13**, 1091 (2017).
[11] S. D. Huber, Nat. Phys. **12**, 621 (2016).
[12] R. Susstrunk and S. D. Huber, Proc. Natl. Acad. Sci. U.S.A. **113**, E4767 (2016).
[13] R. Susstrunk and S. D. Huber, Science **349**, 47 (2015).
[14] L. M. Nash, D. Kleckner, A. Read, V. Vitelli, A. M. Turner, and W. T. M. Irvine, Proc. Natl. Acad. Sci. U.S.A. **112**, 14495 (2015).
[15] P. Wang, L. Lu, and K. Bertoldi, Phys. Rev. Lett. **115**, 104302 (2015).
[16] Y.-T. Wang, P.-G. Luan, and S. Zhang, New J. Phys. **17**, 073031 (2015).
[17] T. Kariyado and Y. Hatsugai, Sci. Rep. **5**, 18107 (2015).
[18] S. R. D. Groot and P. Mazur, *nonEquilibrium Thermodynamics* (Dover Publications, New York, 1962) see in particular CH. XII, § 2.
[19] J. E. Avron, J. Stat. Phys. **92**, 543 (1998).
[20] See Supplemental Material at http://link.aps.org/supplemental/10.1103/PhysRevLett.122.128001 for details of calculations and review of background material.
[21] K. Jensen, M. Kaminski, P. Kovtun, R. Meyer, A. Ritz, and A. Yarom, J. High Energy Phys. 05 (2012) 102.
[22] M. Kaminski and S. Moroz, Phys. Rev. B **89**, 115418 (2014).
[23] F. M. Haehl, R. Loganayagam, and M. Rangamani, Phys. Rev. Lett. **114**, 201601 (2015).
[24] Y. Nakagawa, J. Phys. Earth **4**, 105 (1956).
[25] S. Chapman, T. Cowling, D. Burnett, and C. Cercignani, *The Mathematical Theory of nonuniform Gases: An Account of the Kinetic Theory of Viscosity, Thermal Conduction and Diffusion in Gases*, Cambridge Mathematical Library (Cambridge University Press, Cambridge, England, 1990) see in particular § 19.44.
[26] H. Knaap and J. Beenakker, Physica (Amsterdam) **33**, 643 (1967).
[27] L. Pitaevskii and E. Lifshitz, *Physical Kinetics* (Elsevier Science, New York, 2012), Vol. 10 see in particular § 58 and § 59.
[28] P. Wiegmann and A. G. Abanov, Phys. Rev. Lett. **113**, 034501 (2014).
[29] A. Bogatskiy and P. Wiegmann, arXiv:1812.00763.
[30] A. G. Abanov and G. M. Monteiro, arXiv:1810.04501.
[31] A. G. Abanov, T. Can, and S. Ganeshan, SciPost Phys. **5**, 10 (2018).
[32] D. Banerjee, A. Souslov, A. G. Abanov, and V. Vitelli, Nat. Commun. **8**, 1573 (2017).
[33] G. E. Volovik, Sov. Phys. Usp. **27**, 363 (1984).
[34] J. E. Avron, R. Seiler, and P. G. Zograf, Phys. Rev. Lett. **75**, 697 (1995).
[35] I. V. Tokatly and G. Vignale, Phys. Rev. B **76**, 161305 (2007).
[36] I. V. Tokatly and G. Vignale, J. Phys. Condens. Matter **21**, 275603 (2009).
[37] N. Read, Phys. Rev. B **79**, 045308 (2009).
[38] N. Read and E. H. Rezayi, Phys. Rev. B **84**, 085316 (2011).
[39] M. Barkeshli, S. B. Chung, and X.-L. Qi, Phys. Rev. B **85**, 245107 (2012).
[40] A. Shitade and T. Kimura, Phys. Rev. B **90**, 134510 (2014).
[41] D. Vollhardt and P. Wolfle, *The Superfluid Phases of Helium 3*, Dover Books on Physics (Dover Publications, New York, 2013).
[42] K. Fujii and Y. Nishida, Ann. Phys. (Amsterdam) **395**, 170 (2018).
[43] B. Offertaler and B. Bradlyn, Phys. Rev. B **99**, 035427 (2019).
[44] J. Korving, H. Hulsman, H. Knaap, and J. Beenakker, Phys. Lett. **21**, 5 (1966).
[45] J. Korving, H. Hulsman, G. Scoles, H. Knaap, and J. Beenakker, Physica (Amsterdam) **36**, 177 (1967).
[46] H. Hulsman, E. V. Waasdijk, A. Burgmans, H. Knaap, and J. Beenakker, Physica (Amsterdam) **50**, 53 (1970).
[47] A. I. Berdyugin, S. G. Xu, F. M. D. Pellegrino, R. K. Kumar, A. Principi, I. Torre, M. B. Shalom, T. Taniguchi, K. Watanabe, I. V. Grigorieva, M. Polini, A. K. Geim, and D. A. Bandurin, arXiv:1806.01606.
[48] V. Soni, E. Bililign, S. Magkiriadou, S. Sacanna, D. Bartolo, M. J. Shelley, and W. T. M. Irvine, arXiv:1812.09990v1.

[49] H. So, Prog. Theor. Phys. **74**, 585 (1985).
[50] G. E. Volovik, Sov. Phys. JETP **67**, 1804 (1988).
[51] A. Coste and M. Lüscher, Nucl. Phys. **B323**, 631 (1989).
[52] The odd Navier-Stokes equations are linearized around the state $(\rho, \mathbf{v}) = (\rho_0, 0)$. In a rotating fluid, $\mathbf{v}$ is the velocity in the rotating frame and this state corresponds to rigid-body rotation.
[53] W. T. L. Kelvin, Proc. R. Soc. Edinburgh, Sect. A **10**, 92 (1879).
[54] S. L. Rosenthal, Mon. Weather Rev. **93**, 605 (1965).
[55] T. Matsuno, J. Meteorol. Soc. Jpn. Ser. II **44**, 25 (1966).
[56] M. Yanai and T. Maruyama, J. Meteorol. Soc. Jpn. Ser. II **44**, 291 (1966).
[57] T. Maruyama, J. Meteorol. Soc. Jpn. Ser. II **45**, 391 (1967).
[58] A. E. Gill, *AtmosphereOcean Dynamics* (Academic Press, New York, 1982).
[59] While this paper was under review, we became aware of the preprint Ref. [60], in which the effect of odd viscosity on geophysical waves is discussed.
[60] C. Tauber, P. Delplace, and A. Venaille, arXiv:1812.05488.
[61] G. E. Volovik, *The Universe in a Helium Droplet* (Oxford University Press, Oxford, 2009).
[62] G. E. Volovik, JETP Lett. **90**, 587 (2009).
[63] M. A. Silaev and G. E. Volovik, J. Exp. Theor. Phys. **119**, 1042 (2014).
[64] J. Li, A. F. Morpurgo, M. Buttiker, and I. Martin, Phys. Rev. B **82**, 245404 (2010).
[65] M. G. Silveirinha, Phys. Rev. B **92**, 125153 (2015).
[66] M. G. Silveirinha, Phys. Rev. B **94**, 205105 (2016).
[67] G. Bal, arXiv:1808.07908.
[68] A. P. Schnyder, S. Ryu, A. Furusaki, A. W. W. Ludwig, V. Lebedev, and M. Feigel'man, in *AIP Conference Proceedings* (AIP, College Park, MD, 2009).
[69] J. Dahler and L. Scriven, Nature (London) **192**, 36 (1961).
[70] D. W. Condiff and J. S. Dahler, Phys. Fluids **7**, 842 (1964).
[71] J.-C. Tsai, F. Ye, J. Rodriguez, J. P. Gollub, and T. C. Lubensky, Phys. Rev. Lett. **94**, 214301 (2005).
[72] D. J. Bonthuis, D. Horinek, L. Bocquet, and R. R. Netz, Phys. Rev. Lett. **103**, 144503 (2009).
[73] S. Fürthauer, M. Strempel, S. W. Grill, and F. Jülicher, Eur. Phys. J. E **35**, 89 (2012).
[74] Y. Sumino, K. H. Nagai, Y. Shitaka, D. Tanaka, K. Yoshikawa, H. Chaté, and K. Oiwa, Nature (London) **483**, 448 (2012).
[75] Y. Tabe and H. Yokoyama, Nat. Mater. **2**, 806 (2003).
[76] P. Oswald and G. Poy, Phys. Rev. E **91**, 032502 (2015).
[77] K. Drescher, K. C. Leptos, I. Tuval, T. Ishikawa, T. J. Pedley, and R. E. Goldstein, Phys. Rev. Lett. **102**, 168101 (2009).
[78] A. P. Petroff, X.-l. Wu, and A. Libchaber, Phys. Rev. Lett. **114**, 158102 (2015).
[79] J. Yan, S. C. Bae, and S. Granick, Soft Matter **11**, 147 (2015).
[80] I. Riedel, K. Kruse, and J. Howard, Science **309**, 300 (2005).
[81] J. Denk, L. Huber, E. Reithmann, and E. Frey, Phys. Rev. Lett. **116**, 178301 (2016).
[82] A. Snezhko, Curr. Opin. Colloid Interface Sci. **21**, 65 (2016).
[83] C. Maggi, F. Saglimbeni, M. Dipalo, F. D. Angelis, and R. D. Leonardo, Nat. Commun. **6**, 7855 (2015).
[84] E. Lemaire, L. Lobry, N. Pannacci, and F. Peters, J. Rheol. **52**, 769 (2008).
[85] P. Lenz, J.-F. Joanny, F. Jülicher, and J. Prost, Phys. Rev. Lett. **91**, 108104 (2003).
[86] N. Uchida and R. Golestanian, Phys. Rev. Lett. **104**, 178103 (2010).
[87] K. Yeo, E. Lushi, and P. M. Vlahovska, Phys. Rev. Lett. **114**, 188301 (2015).
[88] M. Spellings, M. Engel, D. Klotsa, S. Sabrina, A. M. Drews, N. H. P. Nguyen, K. J. M. Bishop, and S. C. Glotzer, Proc. Natl. Acad. Sci. U.S.A. **112**, E4642 (2015).
[89] N. H. P. Nguyen, D. Klotsa, M. Engel, and S. C. Glotzer, Phys. Rev. Lett. **112**, 075701 (2014).
[90] B. C. van Zuiden, J. Paulose, W. T. M. Irvine, D. Bartolo, and V. Vitelli, Proc. Natl. Acad. Sci. U.S.A. **113**, 12919 (2016).
[91] M. Han, J. Yan, S. Granick, and E. Luijten, Proc. Natl. Acad. Sci. U.S.A. **114**, 7513 (2017).
[92] M. G. Silveirinha, Phys. Rev. X **9**, 011037 (2019).